



The influence of Li on the thermophysical properties of liquid Ga–Sn–Zn eutectic alloys

A. Dobosz¹ · Yu. Plevachuk² · V. Sklyarchuk¹ · B. Sokoliuk² · T. Gancarz¹

Received: 15 July 2019 / Accepted: 21 September 2019 / Published online: 27 September 2019
© The Author(s) 2019

Abstract

The Ga–Li system is very attractive for the development of microelectronic and Li-ion cell applications as negative electrodes. In this study, thermophysical properties such as density, surface tension, viscosity, thermal and electrical conductivity, and thermoelectric power were investigated. Taking into account the intermetallic compounds occurring in Ga–Li, the measurements were conducted in a temperature range of 323–773 K. The experimentally obtained results revealed lower density and surface tension with increasing Li additions. The viscosity, electrical conductivity and thermoelectric power slightly reduced with the addition of Li content to eutectic Ga–Sn–Zn. The opposite was true of thermal conductivity, which increased slightly. The performed Nusselt number and Peclet number calculations for eutectic Ga–Sn–Zn with Li additions show similar dependency as found in literature data for Ga and Ga–In alloys.

1 Introduction

Increasing energy demand has caused the development of new green energy sources [1] and nuclear power [2]. In the first case, problems connected with energy storage can arise [3], leading to the use of Li-ion batteries which are characterised by high capacity [4]. However, there is poor wetting between molten Li metal and garnet pellets, due to the large difference in surface energy. Therefore, the materials used are very sensitive to temperature changes. High temperatures accelerate degradation and shorten the life of these materials, while low temperatures increase the internal electric resistance of the battery and reduce its efficiency [5]. Thus, a thermal management system, which could control temperature during battery cooling and heating cycles, is needed. The cooling process could be controlled by either air or liquids, however using liquid metal coolants demonstrates a greater efficiency compared to the previously mentioned systems [1]. Liquid metals have been investigated as a successful cooling fluid in high power LEDs, for computer chips and for nuclear plant cooling. Moreover, liquid metals offer

possibilities in terms of the electromagnetic drive, giving them a further advantage for application in cooling systems [5]. The most commonly used liquid metals are based on Ga, offering very good prospects and great potential for application as sensors, coolants, flexible and stretchable electronics, microfluids and self-healing devices [6]. Ga additions have been used in joints in order to reduce the temperature at which the joining process can be conducted [7–9]. In coolants, properties such as thermal conductivity, liquidus temperature, viscosity, density, heat capacity, etc. are crucial for the efficiency and functionality of the cooling system. On the other hand, the dissolution of elements with which the liquid comes into contact will change the abovementioned properties.

Ternary systems based on gallium are interesting as they possess low melting temperatures (lower than unary and binary systems), while still being not extremely complex and are easier to understand than more complicated systems. Ga–In–Sn and Ga–Sn–Zn systems are being the most widely investigated, this work focuses on the later as it replaces indium, which is an expensive element, with more common elements, like tin and zinc. When Li dissolves into Ga–Sn–Zn eutectic, intermetallic compounds with lithium (IMCs) could form, according to the Ga–Li [10] and Ga–Li–Zn [11] phase diagrams. The Li admixtures form IMCs [4, 12–14], which cause an improvement of the mechanical properties, moreover lithium in the case of solid-state Li metal batteries exhibits the lowest reduction

✉ T. Gancarz
tomasz.gancarz@imim.pl

¹ Institute of Metallurgy and Materials Science, Polish Academy of Sciences, Krakow, Poland

² Department of Metal Physics, Ivan Franko National University of Lviv, Lviv 79005, Ukraine

potential and the highest theoretical specific capacity. The greatest demand for Li-ion batteries with liquid metal cooling systems is in electric vehicles, where the principle of self-welding could make it easier to seal cracks in the coolant system [5]. In alkali metals, self-welding on the basis of the diffusion bond is clearly manifested [15]. Hence, if two contacting pieces of solid metal are immersed in sodium at a temperature of about 500 K or higher, they will be tightly connected after a while. Lithium has similar properties. In this case, the liquid metal makes it easier to transfer atoms from one solid to another. On this principle, it is possible to seal cracks in the coolant circuit, making the system more reliable.

This study is focused on the thermophysical properties of eutectic Ga–Sn–Zn with Li additions. Taking into account the potential application in batteries, this investigation shows the effect of Li additions, which could be dissolved into the coolant, on density, surface tension, viscosity, thermal and electrical conductivity, and thermoelectric power. The temperature dependency for these properties is presented for different Li content in eutectic Ga–Sn–Zn. The obtained results were compared with literature data for Ga–Sn [16], Ga–Zn [17], Ga–Sn–Zn [18] and Ga–In–Sn [19], and with the previously studied properties of eutectic Ga–Sn–Zn with Al [20], In [21] and Bi [22] additions.

2 Experimental

This study investigated the properties of eutectic Ga–Sn–Zn alloys (90.1 Ga, 6.8 Sn and 3.1 Zn (at.)) with 0.01, 0.05, 0.1, 0.5 and 1.0 (wt%) Li, which corresponds to 0.1, 0.52, 1.04, 5.01 and 9.59 (at.%) Li. Due to the reactivity of Li, the alloys were prepared in a glove-box with high purity Ar (99.9999%) atmosphere, with levels of H₂O and O₂ below 1 ppm, and the N₂ amount significantly lowered. For preparation of the alloys, high purity metals Ga (99.99999%) from PPM Pure Metals, and Sn and Zn (99.999%) from Alfa Aesar, were used. The appropriately weighted amounts of each component were melted in graphite crucibles, which were placed directly in a resistance furnace. As mentioned above, the melting and handling of the alloys was done in a glove-box. All experiments were conducted by heating to the highest temperature possible for each measurement, followed by a step by step cooling. Differential scanning calorimetry (DSC) and thermal mechanical analysis (TMA) were carried out to determine solidification and melting temperatures (collected in Table 1). In the DSC measurements, the heating rate was 10 K/min with an Ar protective atmosphere. The thermal linear coefficient (CTE) was determined with a heating and cooling rate of 2 K/min with He protective atmosphere. To determine density, viscosity and surface tension, the discharge crucible method (DC) was used, as

Table 1 Chemical composition, melting and solidification temperature and CTE of studied alloys

Alloys	Al additions		Temperature		CTE
	wt%	at.%	Solidification	Melting	
Ga–Sn–Zn [18]			267.5	288.1	109
Ga–Sn–Zn0.01Li	0.01	0.10	280.6	299.4	106
Ga–Sn–Zn0.05Li	0.05	0.52	278.2	300.0	107
Ga–Sn–Zn0.1Li	0.10	1.04	281.1	302.2	110
Ga–Sn–Zn0.5Li	0.50	5.01			
Ga–Sn–Zn1.0Li	1.00	9.59			

described in details in other works [8, 23–25]. The method consists of allowing the free flow of the liquid alloy through a hole at the bottom of a graphite crucible, which rests on a set of scales, allowing for an accurate measurement of the weight. The method requires calibration, which was performed using pure metal [23], to obtain density, surface tension and viscosity, which can be calculated based on the measured changes in weight over a given period of time, as shown in Eq. (1). The relationship between the volumetric flow rate of liquid Q exiting the crucible through the orifice of fixed radius r_0 , the head of the liquid, is calculated using Eq. (1):

$$h = \frac{1}{2g} \left[\frac{Q}{\left(a_4 \left(\frac{2\rho Q}{\pi r_0 \eta} \right)^3 + a_3 \left(\frac{2\rho Q}{\pi r_0 \eta} \right)^2 + a_2 \left(\frac{2\rho Q}{\pi r_0 \eta} \right) + a_1 \right) \pi r_0^2} \right] + \frac{\gamma}{\rho g r_0} \quad (1)$$

where: ρ is the density of liquid (kg/m³), g denotes gravitational acceleration (m/s²), r_0 is the radius of the orifice in the bottom of crucible (m), σ is surface tension (mN/m), Q is free flow (m³/s), η and γ are viscosity and surface tension, respectively, and a_1 , a_2 , a_3 and a_4 are constants in the polynomial describing C_d versus Re , Reynolds number [26]. The uncertainty of the measurement of density, viscosity and surface tension is up to 3%. Density and surface tension were described in this work by linear equations, while the viscosity was characterized by an Arrhenius equation. Tables 2, 3, and 4 present the mentioned thermophysical data taken at 573 K, with estimated standard deviation of the parameters of the equation. The density and surface tension line, as well as the Arrhenius equation which described the viscosity fit excellently to the experimental data, and the parameter R^2 was in the range of 0.991–0.999.

Electrical conductivity and thermoelectric power measurement were performed in argon atmosphere using the contact four-probe method, the experimental setup of which is described in [27]. The temperature dependency of electrical conductivity and thermoelectric power were measured

Table 2 Coefficients^a and standard deviation^b of the temperature dependency of density, as described by the linear equation $\rho = A + B \cdot T$ for eutectic Ga–Sn–Zn alloys with Li additions, and the corresponding density values, calculated at 573 K^c. ++

Ga–Sn–Zn–Li X _{Li} (wt%)	A (g cm ⁻³)	u (A)	B (g cm ⁻³ K ⁻¹)	u (B)	ρ (573 K) (g cm ⁻³)	s (ρ)
Ga–Sn–Zn _{eut} [18]	6.332		–0.00061		5.983	
0.01	6.097	0.005	–0.00060	0.00001	5.753	0.004
0.05	5.894	0.007	–0.00059	0.00001	5.555	0.005
0.1	5.683	0.008	–0.00058	0.00001	5.351	0.004
Li [31]	0.563		–0.00010		0.506	

^aValues estimated from linear regression error as implemented in the Grapher Software Package

^bValues estimated from the difference computed between experimental and calculated from linear density fit, $s(m) = \frac{1}{N} \sum_{i=1}^N |m^{\text{exp}} - m^{\text{fit}}|$, where N is the number of experimental points and standard deviation of density $s(\rho)$

^cStandard uncertainties u are u(T)=1 K, u(p)=0.1 kPa at atmospheric pressure p=0.1 MPa, u(X)=0.01 for Li, Ga, Sn and Zn

Table 3 Coefficients^a and standard deviation^b of temperature dependency of surface tension, as described by the linear equation $\gamma = A + B \cdot T$ for eutectic Ga–Sn–Zn alloys with Li additions, and the corresponding surface tension values, calculated at 573 K^c

Ga–Sn–Zn–Li X _{Li} (wt%)	A (mN m ⁻¹)	u (A)	B (mN m ⁻¹ K ⁻¹)	u (B)	γ (573 K) (mN m ⁻¹)	s (γ)
Ga–Sn–Zn _{eut} [18]	716.5		–0.074		674.1	
0.01	710.6	0.3	–0.075	0.001	667.5	0.248
0.05	703.7	0.5	–0.077	0.001	659.6	0.340
0.1	695.9	0.7	–0.078	0.001	651.4	0.366
Li [34]	461.9		–0.140		381.2	

^aValues estimated from linear regression error as implemented in the Grapher Software Package

^bValues estimated from the difference computed between experimental and calculated from linear surface tension fit, $s(m) = \frac{1}{N} \sum_{i=1}^N |m^{\text{exp}} - m^{\text{fit}}|$, where N is the number of experimental points and standard deviation of surface tension $s(\gamma)$

^cStandard uncertainties u are u(T)=1 K, u(p)=0.1 kPa at atmospheric pressure p=0.1 MPa, u(X)=0.01 for Li, Ga, Sn and Zn

Table 4 Coefficients^a (A, E_a) and standard deviation^b of temperature dependency of viscosity, as described by Arrhenius relation ($\eta = A \cdot \exp(E_a/R \cdot T)$) for eutectic Ga–Sn–Zn alloys with Li additions, and the corresponding viscosity values, calculated at 573 K^c

Ga–Sn–Zn–Li X _{Li} (at.%)	A (mPa s)	u (A)	E _a (J mol ⁻¹)	u (E _a)	η (573 K) (mPa s)	s (η)
Ga–Sn–Zn _{eut} [18]	0.376		–3824.3		0.839	
0.01	0.373	0.002	–3836.4	69.3	0.834	0.002
0.05	0.357	0.002	–3938.7	70.8	0.816	0.004
0.1	0.350	0.002	–3961.2	74.5	0.804	0.004
Li [31]	0.146		–5560.0		0.468	

^aValues estimated from linear regression error as implemented in the Grapher Software Package

^bValues estimated from difference computed between experimental and calculated from viscosity fit, $s(m) = \frac{1}{N} \sum_{i=1}^N |m^{\text{exp}} - m^{\text{fit}}|$, where N is the number of experimental points and standard deviation of viscosity $s(\eta)$

^cStandard uncertainties u are u(T)=1 K, u(p)=0.1 kPa at atmospheric pressure p=0.1 MPa, u(X)=0.0001 for Li, Ga, Sn and Zn

simultaneously, which was made possible as a result of the special construction of the crucible and the placement of the heater elements. The uncertainty of measurement of electrical conductivity using the above mentioned method is reported to be 2%, and does not exceed 5%. Thermal conductivity was determined using the steady state concentric cylinder technique, which can be found in details in [28]. The method yields an uncertainty that does not exceed 7%.

3 Results and discussion

The prepared alloys of eutectic Ga–Sn–Zn alloys with 0.01, 0.05 and 0.1 (wt%) additions of Li were liquid at room temperature. Those with higher Li content (0.5 and 1.0 (wt%)) were solid, which is in line with the Ga–Li phase diagram [10]. The measured temperatures

of solidification and melting are collected in Table 1. The obtained experimental results show that the temperature of solidification and melting increase slightly with increasing Li content. The samples with 0.5 and 1.0 (wt%) Li showed the highest values, at 469 and 503 K, respectively, but the liquidus temperature was much higher. The shift of the peak should be taken into account, given that the samples are liquid and dissolution could change the melting temperature of particles corresponding to the occurring phases. From calorimetry study of eutectic Ga–Sn–Zn samples with a higher amount of Li (shown in Fig. 1), which are solid at room temperature, it is evident that high-temperature IMCs from the Ga–Li [10], Sn–Li [29] and Li–Zn [30] systems form in alloys with Li content of 0.5 and 1.0 (wt%). The obtained calorimetry curve, presented in Fig. 1, shows the initial Ga–Sn–Zn dissolution with 0.5 and 1.0 (wt%) Li from 373 K, in accordance with the Li–Sn system. After 523 K, the IMCs from the Ga–Li, Li–Sn and Li–Zn systems are dissolving, in order to dissolve LiGa phase, the sample has to be heated up to around 973 K. It is worth noting that eutectic Ga–Sn–Zn and eutectic Ga–Sn–Zn with 0.01, 0.05, and 0.1 (wt%) Li content alloys were liquid at room temperature and did not show the dependency presented in Fig. 1 for the alloys with higher Li content.

The calculated CTE reduced slightly with increasing Li content in Ga–Sn–Zn, at 107, 106 and 110 (10^{-6} K^{-1}), compared to 109 (10^{-6} K^{-1}) for eutectic Ga–Sn–Zn [18]. The obtained data can be compared with the CTE of Ga–In–Sn which in the temperature range 323–773 K is equal to 147 (10^{-6} K^{-1}) [19]. As in the case of Al additions to eutectic Ga–Sn–Zn [20], the CTE decrease with the content of alloying elements is small, which is correlated with a closer match in the liquid phase. Increasing additions of alloying

elements to eutectic Ga–Sn–Zn caused the formation of IMCs, which is correlated with short ordering in the liquid that corresponds to a higher CTE value. The obtained results are important in the case of cooling systems with lithium, where this element could dissolve into the liquid coolant—the amount of lithium in the Ga–Sn–Zn eutectic limits the low working range of temperatures of the liquid metal.

The temperature dependency of density for eutectic Ga–Sn–Zn alloys with 0.01, 0.05, and 0.1 (wt%) Li is

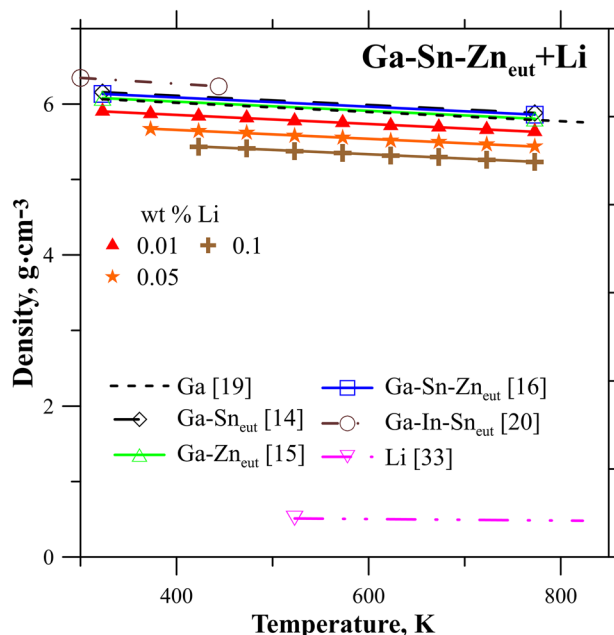
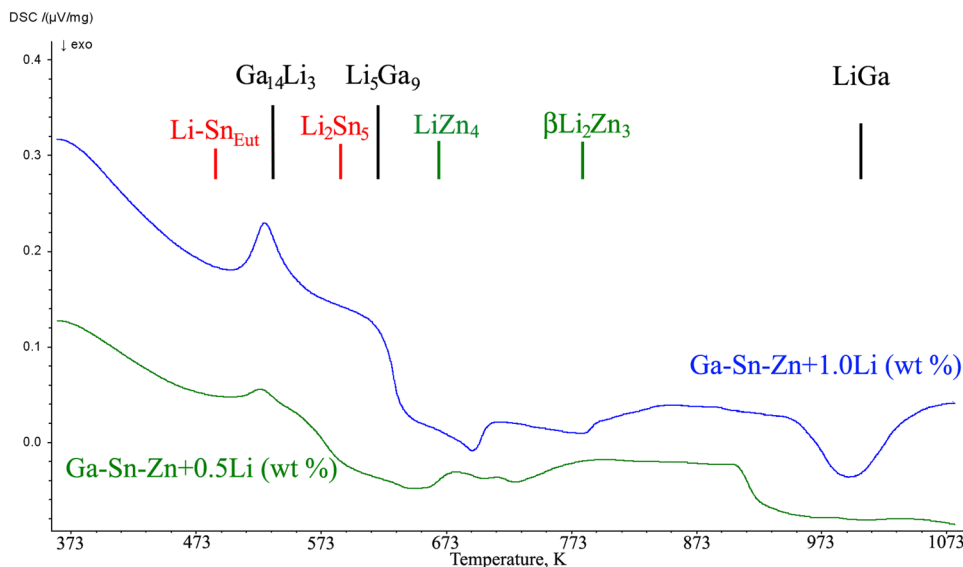


Fig. 2 Density measurement in a function of temperature for eutectic Ga–Sn–Zn with Li additions compared with Ga [32], Li [33], Ga–Sn [16], Ga–Zn [17], Ga–Sn–Zn [18] and Ga–In–Sn [19] literature data

Fig. 1 Calorimetry curves measured for eutectic Ga–Sn–Zn alloy with 0.5 and 1.0 (wt%) Li



presented in Fig. 2. The density values are reduced with increasing temperature and Li content. The obtained experimental results for Ga–Sn–Zn–Li alloys are lower compared to those for eutectic Ga–Sn–Zn [18] and Ga–In–Sn [19]. Similarly for the previously investigated Al addition [20] the density values decrease with higher amount of Al, in the case of Li, the lowest density value was observed for 0.1 (wt%) of Li. The density value of elemental Li is equal to $0.506 \text{ (g.cm}^{-3}\text{)}$ [31] and is one order of magnitude less than values for eutectic Ga–Sn–Zn $5.983 \text{ (g.cm}^{-3}\text{)}$ at a temperature of 573 K, which has a high impact on density results of the studied alloys. A trend of decreasing density with Li content, such as for eutectic ZnAl with Li additions [25] was observed. In [25], the reduction in density was caused by the formation of IMCs from the Al–Li and Li–Zn systems [12]. In the case of this work, there is a similar association with the liquid from short-range ordering caused by IMCs, as was observed for higher Li content (Fig. 1). The obtained temperature dependency of density for eutectic Ga–Sn–Zn with Li additions was described using a linear type equation ($\rho = A + BT$). The coefficients of the equation, as well as the errors associated with them, are shown in Table 2. The obtained parameters A and B, and density values, reduce with increasing Li content.

Surface tension versus temperature for eutectic Ga–Sn–Zn with Li additions is presented in Fig. 3. The obtained results for surface tension show reducing values with increasing Li content. For 1.0 (wt%) Li, the obtained results are close to

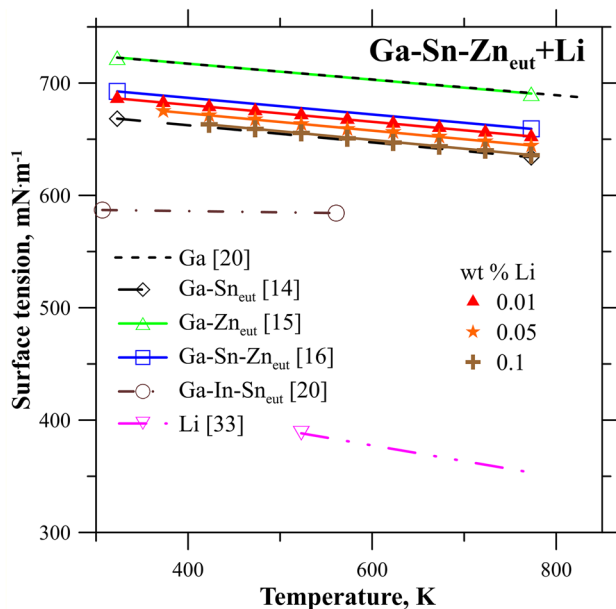


Fig. 3 Surface tension measurement in a function of temperature for eutectic Ga–Sn–Zn with Li additions compared with Ga [32], Li [33], Ga–Sn [16], Ga–Zn [17], Ga–Sn–Zn [18] and Ga–In–Sn [19] literature data

those for eutectic Ga–Sn [16]. As observed for Bi additions [22] to eutectic Ga–Sn–Zn, the Li content also reduces surface tension. The results in this case were $633.8 \text{ (mN m}^{-1}\text{)}$ for 5 (wt%) Bi and $651.4 \text{ (mN m}^{-1}\text{)}$ for 0.1 (wt%) Li, at the temperature of 573 K. The reducing surface tension is correlated with Li additions, for which surface tension is much lower [32]. The Li additions in the liquid segregate to the surface, causing lower surface tension. Moreover, the Ga-based alloys have a tendency towards oxidation due to gallium properties and the Li additions should intensify this phenomenon. However, it can be noted that oxidation can be a positive effect and was already used in order to produce thin 2D oxide layers [33]. The process of fabrication of such layer can be undertaken at room temperature. In the case of a cooling system for lithium batteries, it may be important to limit the amount of oxygen that could come in contact with the liquid metal coolant. The obtained surface tension results for Ga–Sn–Zn with Li content were described using a linear equation ($\gamma = A + B \cdot T$). The coefficients of the mentioned equation, the errors connected to them, as well as the calculated value of surface tension at 573 K, are shown in Table 3.

The temperature dependency of viscosity for eutectic Ga–Sn–Zn alloy with Li additions is presented in Fig. 4. The experimental results were compared with literature data for Ga [32], Ga–Sn [16], Ga–Zn [17], Ga–Sn–Zn [18] and Ga–In–Sn [19]. The addition of Li content to the base alloy resulted in a slight decrease of viscosity. The viscosity values for the addition of 0.01 (wt%) Li were at the same

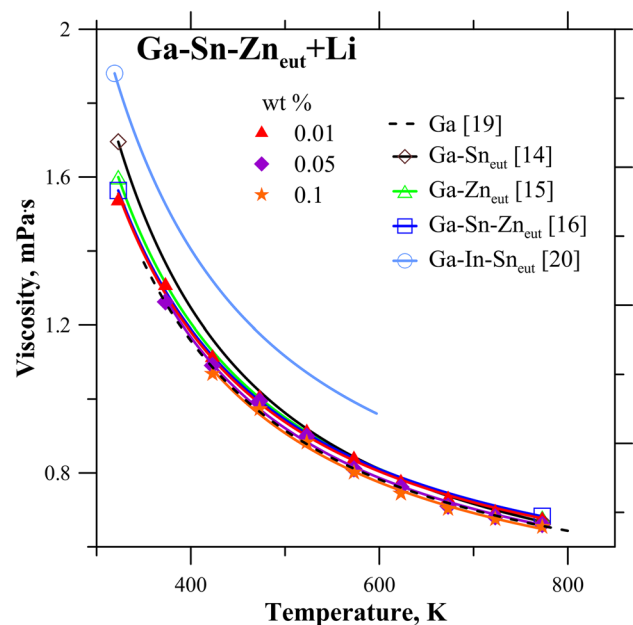


Fig. 4 Viscosity measurement in a function of temperature for eutectic Ga–Sn–Zn with Li additions compared with Ga [32], Ga–Sn [16], Ga–Zn [17], Ga–Sn–Zn [18] and Ga–In–Sn [19] literature data

level as for those for eutectic Ga–Zn [17] and Ga–Sn–Zn [18]. Li content of 0.05 and 0.1 (wt%) lowered the values in comparison to those of pure Ga [30]. The obtained experimental results for viscosity were described by an Arrhenius type equation ($\eta = A \exp(E_a/RT)$). The coefficients of the equation, along with the standard deviation, are collected in Table 4. From the Arrhenius equation, the activation energies have been determined. It was observed that the activation energy increases with increasing Li content in eutectic Ga–Sn–Zn. The small amount of Li caused viscosity to decrease, while higher Li content could be associated with increasing viscosity, which is correlated with IMC formation as observed in the calorimetry curve (Fig. 1) and the short-range ordering in the case of ZnAl with Li alloys [25]. Therefore, the low Li content dissolves in Ga, which is in line with the Ga–Li phase diagram, causing reduced viscosity due to the lower viscosity of pure Li 0.486 (mPa.s) at the temperature of 573 K [33]. It should be pointed out that lower values of viscosity are beneficial for cooling systems, as less energy is required in order for the liquid to flow through the cooling system. An increase of viscosity, as is the case of a high amount of lithium dissolved in the base eutectic Ga–Sn–Zn alloy, has to be taken into account and eliminated if possible by avoiding the risk of a too high amount of lithium dissolving into the cooling liquid.

Three Ga–Sn–Zn samples with 0.01, 0.05, 0.1 wt% additions of lithium were selected for the investigations of electrical conductivity. The measurements were carried out in a wide temperature range beginning from the melting temperatures of each alloy, which were determined from the calorimetry curves (Table 1) up to 900 K. The measurement were performed during heating and subsequent cooling. Temperature dependencies of electrical conductivity for all investigated liquid alloys as well as for their constituent elements Ga [19], Sn [35], Zn [36] and Li [37] are presented in Fig. 5.

Similarly to other molten metal alloys (see [38] and references therein), the first $\sigma(T)$ curve was not smooth, reflecting numerous structural transformations which occur during first heating starting from the initial microheterogeneous state just above the melting point and the consequent homogeneous solution which is present at high temperatures.

Temperature dependence of electrical conductivity is well described by the following polynomial:

$$\sigma(T) = \sigma_0 + a \cdot (T - T_m) + b \cdot (T - T_m)^2, \quad (2)$$

where σ_0 denotes the electrical conductivity at the melting temperature T_m , and a , b are fitting coefficients, as presented in Table 5.

As reported in [18, 38], the shape of the $\sigma(T)$ curve in a multicomponent liquid alloy depends on the influence of the electrical conductivities of its constituent elements. Comparing

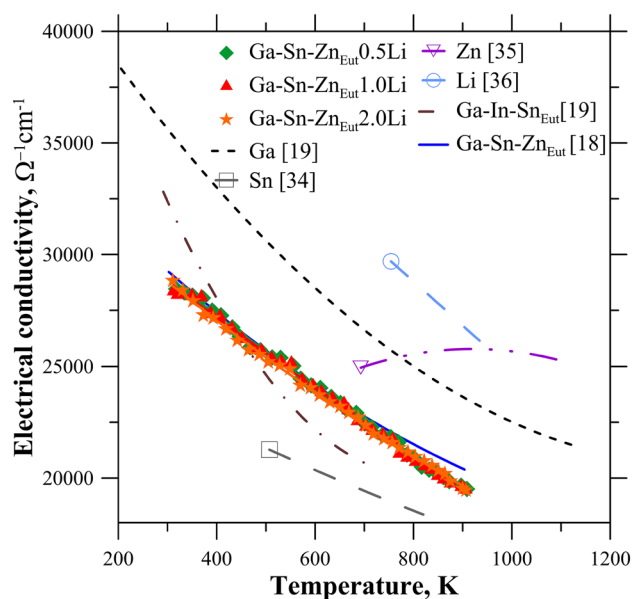


Fig. 5 Electrical conductivity measurement for the eutectic Ga–Sn–Zn eutectic alloy with 0.01, 0.05 and 0.1 (wt%) of Li additions, the lines the polynomial fits, this work. The dotted lines represent literature data: Li [37], Ga [19], Sn [35], Zn [36] and Ga–In–Sn_{eut} [19] are shown for comparison

the non-linear $\sigma(T)$ curve of Ga–Sn–Zn, which is formed as a result of the linear $\sigma(T)$ curve of liquid tin [35], being slightly concave in liquid Ga [19] and convex one in liquid Zn [36, 39], the $\sigma(T)$ dependence in liquid eutectic Ga–Sn–Zn alloys with Li additions is more linear. The electrical conductivity of liquid lithium has a linear temperature dependence [37], which we believe has an insignificant effect on the overall electrical conductivity in the studied case.

The absolute values of the measured electrical conductivity of Ga–Sn–Zn+Li alloys are slightly lower than those of Ga–Sn–Zn. Solutions of Li in Ga, Sn, Zn form the alloys belonging to systems with strong interaction between the components. The phase diagrams of those systems reveal a number of intermetallic or chemical compounds of covalent or ionic nature ($\text{Ga}_{14}\text{Li}_3$, Ga_2Li , Ga_4Li_5 and GaLi), as mentioned before. It can be assumed that an area of ordering in the size of one or more coordination spheres is formed between the components around the impurity particle, and this complex is present in the melt as a more or less stable formation. This may lead to a decrease in the effective concentration of conduction electrons. The scattering of electrons can be quite large. The large cross-sections of electron scattering lead to a decrease in electrical conductivity. This σ reduction, marked as $\Delta\sigma_i$, can be found from the following equation:

$$\Delta\sigma_i^{-1} = N_i \frac{m v_F}{e^2} \Sigma_i \quad (3)$$

Table 5 Electrical conductivity, σ_0 , and coefficients T_m , a , b as from Eq. (4) describing the temperature dependence of electrical conductivity for eutectic Ga–Sn–Zn alloys with Li additions

Alloy composition (wt%)	T_m (K)	σ_0 (Ohm ⁻¹ cm ⁻¹)	a (Ohm ⁻¹ cm ⁻¹ K ⁻¹)	b (Ohm ⁻¹ cm ⁻¹ K ⁻²)
Ga–Sn–Zn [16]	288.1	29,503	– 19,4776	0.0076
Ga–Sn–Zn _{Eut} 0.01Li	300	28,918	– 16.4334	0.0012
Ga–Sn–Zn _{Eut} 0.05Li	302.2	28,746	– 15.9667	0.0005
Ga–Sn–Zn _{Eut} 0.1Li	303.6	28,720	– 17.635	0.0041

where N_i is the atomic fraction of impurities, m stands for the electron mass, e denotes the charge of the electron charge, v_F is the electron velocity at the Fermi level and Σ_i is a scattering cross-section of the conducting electrons at the particles of impurities.

The electrical conductivity reduction can be also determined from the Linde rule:

$$\Delta\sigma_i^{-1} = N_i[a + b(\Delta Z)^2], \quad (4)$$

where a and b are constants for a given solvent metal and a given row in the periodical table and Z is the valence difference. For the admixtures of normal metals, Linde's rule turns out to be valid for binary and also ternary alloys. Thus, although the electrical conductivity of the elemental lithium is essentially higher than the conductivity of the other alloy components, the Li admixtures do not increase the common conductivity of the Ga–Sn–Zn eutectic alloys with Li additions.

The thermal conductivity is a crucial parameter in the case of application of any material in a cooling system. The dependency on temperature, $\lambda(T)$, of the liquid eutectic Ga–Sn–Zn alloy with additions of 0.01, 0.05 and 0.1 (wt%) of Li was measured across a temperature range between the melting points of each of the mentioned alloys and approximately 900 K. As seen in Fig. 6, the thermal conductivity of all investigated alloys increases upon heating in a non-linear manner.

The absolute values for thermal conductivity of Ga–Sn–Zn eutectic alloy with Li admixtures are very close to the $\lambda(T)$ data obtained for the ternary Ga–Sn–Zn eutectic alloy, and do not exceed the interval of experimental uncertainty. If lithium dissolves into the liquid metal coolant during thermal management of a batteries, according to the obtained results the thermal conductivity will not be strongly affected, which in consequence allows for a continued work of the system. It was determined that the thermal conductivity $\lambda(T)$ data, obtained from the experimental $\sigma(T)$ results using the Wiedemann–Franz–Lorenz law, are in accordance with the experimental $\lambda(T)$ data. $\lambda(T)$ dependency can be described by the polynomial:

$$\lambda(T) = \lambda_0 + c \cdot (T - T_m) + d \cdot (T - T_m)^2, \quad (5)$$

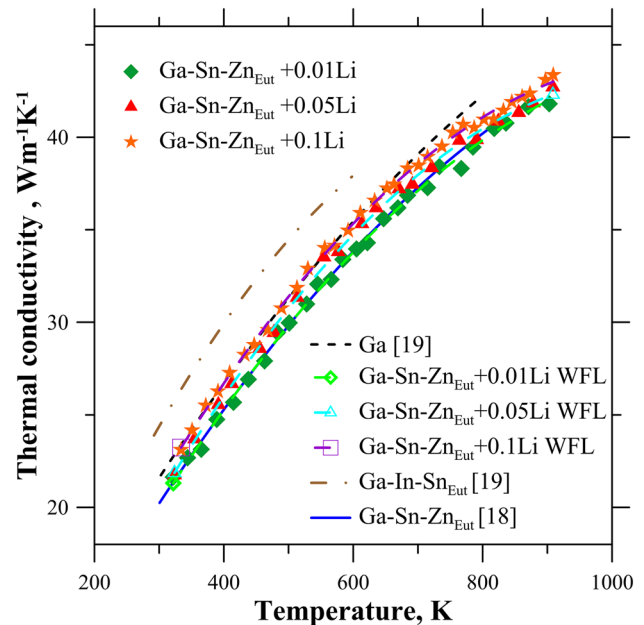


Fig. 6 Thermal conductivity measurement for the Ga–Sn–Zn eutectic alloy with 0.01, 0.05 and 0.1 (wt%) of Li additions. Dashed lines are the values calculated from electrical conductivity $\sigma(T)$ by the Wiedemann–Franz–Lorenz law, while a solid line denotes a polynomial fit. The results are compared with the literature data for Ga [19], Ga–Sn–Zn_{eut} [18] and Ga–In–Sn_{eut} [19]

where λ_0 is the thermal conductivity at the melting temperature T_m , and c and d are fitting coefficients, collected in Table 6.

The simultaneous measurement of the thermoelectric power, S , was performed with the determination of the electrical conductivity of liquid eutectic Ga–Sn–Zn alloy alloyed with 0.01, 0.05 and 0.1 (wt%) of Li. The experiment was conducted during heating and cooling in the mentioned temperature range. The temperature dependency $S(T)$ of the Ga–Sn–Zn–Li alloys is shown in Fig. 7. It has already been demonstrated in previous works [11] that the thermoelectric power of Ga–Sn–Zn decreases slightly when the sample is heated, and this relationship can be characterised by the following polynomial:

$$S(T) = 6.3949 - 0.0318 T + 4.1456 \cdot 10^{-5} T^2 - 1.9682 \cdot 10^{-8} T^3 \quad (6)$$

Table 6 Thermal conductivity λ_0 , and coefficients T_m , c , d from Eq. (7) describing the temperature dependence of thermal conductivity for eutectic Ga–Sn–Zn alloys with Li additions

Alloy composition (wt%)	T_m (K)	λ_0 (W m ⁻¹ K ⁻¹)	c	d
Ga–Sn–Zn [16]	288.1	19.5664	0.0541	–2.6978E–005
Ga–Sn–Zn _{Eut} 0.01Li	300.0	20.1279	0.0546	–3.0358E–005
Ga–Sn–Zn _{Eut} 0.05Li	302.2	20.6317	0.0585	–3.7498E–005
Ga–Sn–Zn _{Eut} 0.1Li	303.6	21.5273	0.0572	–3.5917E–005

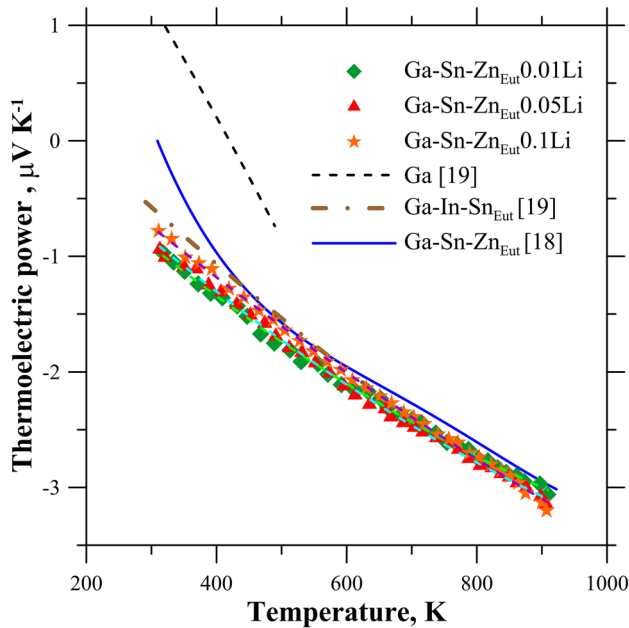


Fig. 7 Thermoelectric power measurement for the liquid Ga–Sn–Zn eutectic alloy with 0.01, 0.05 and 0.1 (wt%) of Li additions. The solid line is a polynomial fit. The results are compared with literature data for Ga [19], Ga–Sn–Zn_{eut} [18] and Ga–In–Sn_{eut} [19]

Small additions of Li result in a less sloping $S(T)$ curves. Thus the following second-order polynomials can describe the temperature dependency of the thermoelectric power measured in this experiment:

$$S(T) = S_0 + e \cdot (T - T_m) + f \cdot (T - T_m)^2, \tag{7}$$

where S_0 is the thermoelectric power at the melting temperature T_m , and e and f are fitting coefficients, which are presented in Table 7.

Table 7 Thermoelectric power S_0 , and coefficients T_m , e , f from Eq. (9) describing the temperature dependence of thermoelectric power for eutectic Ga–Sn–Zn alloys with Li additions

Alloy composition (wt% Li)	T_m (K)	S_0 (μV K ⁻¹)	e	f
Ga–Sn–Zn _{Eut} 0.01Li	300	–0.9169	–0.0044	1.5901E–006
Ga–Sn–Zn _{Eut} 0.05Li	302.2	–0.8678	–0.0046	1.5725E–006
Ga–Sn–Zn _{Eut} 0.1Li	303.6	–0.7585	–0.0045	9.4665E–007

As in the case of the eutectic Ga–Sn–Zn melt, the thermoelectric power values of all Ga–Sn–Zn–Li alloys are negative in the investigated temperature range, keeping the negative dS/dT slope. An increase of Li content leads to a negligible decrease of S .

3.1 Heat transfer simulation

A heat transfer simulation was conducted in order to further understand the potential of Ga–Sn–Zn eutectic alloy as an effective coolant in thermal management systems.

The Nusselt number (Nu) was determined as a function of the Peclet number (Pe) for the Ga–Sn–Zn alloy. The Nusselt number can be used to determine the heat transferred between a coolant and a heating surface, which is a crucial parameter in the case of gallium-based alloys investigated in this regard. The most significant correlations used to calculate the Nusselt number were developed by Martinelli and Lyon [40, 41], and Seban and Shimazaki [42]. Lubrasky and Kaufman provided another empirical equation for the description of the correlation between Nu and Pe [42]. The equations used in this work to model the relation between the mentioned parameters are shown below Lyon [42], Seban and Shizamaki [43], and Lubarsky and Kaufman [44]:

$$Nu = 7 + 0.025Pe^{0.8} \tag{8}$$

$$Nu = 5 + 0.025Pe^{0.8} \tag{9}$$

$$Nu = 0.625Pe^{0.4} \tag{10}$$

The Peclet number was calculated using available experimental data using Eq. (11).

$$Pe = Re \cdot \frac{Cp \cdot \eta}{\lambda} \tag{11}$$

where Re is the Reynolds number, C_p is heat capacity, η is the viscosity of the alloy, and λ is the thermal conductivity.

Figure 8 presents the correlation between the Nusselt and Peclet numbers. The obtained model correlations for Ga–Sn–Zn alloy are compared with experimental literature data concerning pure gallium and Ga15In alloy [44]. Moreover, the experimental data obtained in [45] for Bi–Pb alloys is also shown.

Due to very small differences between data for viscosity and thermal conductivity for eutectic Ga–Sn–Zn and eutectic Ga–Sn–Zn with Li additions, the obtained calculation of Nu and Pe for eutectic Ga–Sn–Zn is presented in Fig. 8. As in the case of Sarafraz et al. [44] for Ga and Ga–In alloys, the obtained data of Nu and Pe for eutectic Ga–Sn–Zn and eutectic Ga–Sn–Zn with Li additions were in the same range. The obtained differences of Nu vs Pe result from different methods of calculating Nu , proposed by Lyon [42], Seban and Shizamaki [43], and Lubarsky and Kaufman [44]. However, as presented in [44], when experimental data are compared with the model for pure Ga, the Seban and Shimazaki model [43] shows the best fit. For Ga–In alloys with higher In content, the Lyon model [42] is best. Taking into account the performed calculation for eutectic Ga–Sn–Zn and eutectic Ga–Sn–Zn with Li additions, it should be assumed that the Lyon model provides the better description [43].

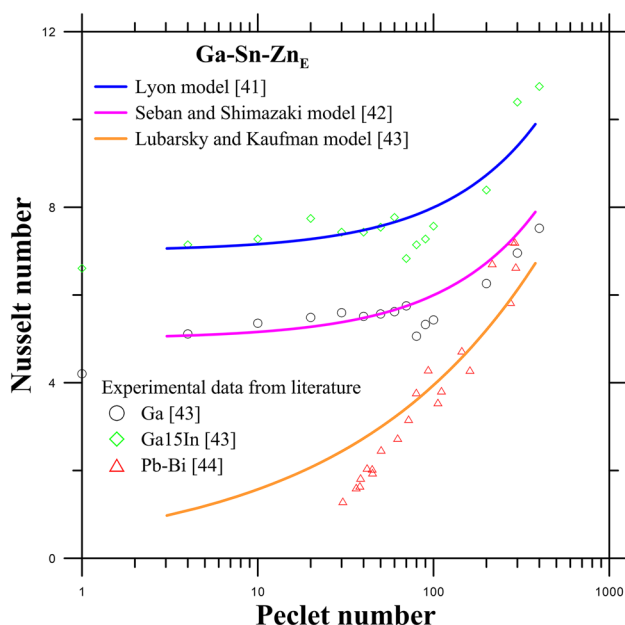


Fig. 8 Correlation between the Nusselt number and Peclet number, with literature data for Ga [43], Ga15In [43] and Pb–Bi [44]

4 Conclusions

This study has investigated the effect of small additions of Li to eutectic Ga–Sn–Zn on thermophysical properties such as density, surface tension, viscosity, electrical and thermal conductivity and thermoelectric power. Taking into account the potential applications of liquid metals in cooling systems for batteries based on Li, effects such as Li dissolution in the proposed liquid metal coolant are very important. During the experiments, the following was determined:

- Alloys with higher Li content (0.5 and 1.0 (wt%)) in eutectic Ga–Sn–Zn alloy show higher liquidus temperatures, caused by the formation of high-temperature phases from the Li–Ga, Li–Sn and Li–Zn systems. For lower Li content (below 0.5 (wt%)), the effect of dissolving high-temperature phases was not observed and the coolant could still operate in the lower temperature range.
- The obtained results for density, surface tension and viscosity show that small additions (0.05, 0.01 and 0.1 (wt%)) of Li to eutectic Ga–Sn–Zn cause the values of these properties to decrease. This could be correlated with the solubility limit of Li in the investigated alloys, with small Li additions fitting in this range.
- Although the electrical conductivity of elemental lithium is essentially higher than the conductivity of other alloy components, the Li admixtures do not increase the common conductivity of the Ga–Sn–Zn + Li alloys. The electrical conductivity of all investigated Ga–Sn–Zn + Li alloys is slightly lower than the conductivity of the Ga–Sn–Zn eutectic alloy. The obtained results confirm the assumption that the addition of admixtures decreases the electrical conductivity, and the Linde rule, which is valid for a number of binary liquid alloys, can also be suitable for systems with more components.
- The thermal conductivity of all investigated alloys increases non-linearly with rising temperatures. The corresponding values calculated from the electrical conductivity are consistent with experimental findings within the range of experimental uncertainty. The absolute values of thermal conductivity of Ga–Sn–Zn eutectic alloy with Li admixtures are very close to λ data of ternary Ga–Sn–Zn, and do not exceed the interval of experimental uncertainty.
- The thermoelectric power of all Ga–Sn–Zn_E + Li alloys remains negative across the entire temperature interval of the liquid state, similar to $S(T)$ of the Ga–Sn–Zn alloy. An increase of Li content leads to a very negligible decrease of S .
- Small admixtures of lithium (up to 0.5 (wt%)) do not have a noticeable effect on the electrophysical properties of the Ga–Sn–Zn eutectic alloy.

In summary, taking into account all the investigated properties, small Li additions to eutectic Ga–Sn–Zn have an inconsiderable effect, which gives very good prospects for the application of liquid metals in battery cooling system. In systems where liquid metal are used as the main coolant, the temperature distribution is easier to control and stabilise, and as demonstrate in this work efficient materials such as liquid metals based on eutectic Ga–Sn–Zn could be successfully employed.

Acknowledgment This work was financed by the National Science Centre Poland Grant 2016/21/B/ST8/00324 “Design and physicochemical, thermal properties of low temperature metal alloys based on gallium” in 2017–2019.

Open Access This article is distributed under the terms of the Creative Commons Attribution 4.0 International License (<http://creativecommons.org/licenses/by/4.0/>), which permits unrestricted use, distribution, and reproduction in any medium, provided you give appropriate credit to the original author(s) and the source, provide a link to the Creative Commons license, and indicate if changes were made.

References

- N. Lorenzin, A. Abanades, A review on the application of liquid metals as heat transfer fluid in concentrated solar power technologies. *Int. J. Hydrog Energy* **41**, 6990–6995 (2016). <https://doi.org/10.1016/j.ijhydene.2016.01.030>
- M.K. Rowiński, T.J. White, J. Zhao, Small and medium-sized reactors (SMR): a review of technology. *Renew. Sustain. Energy Rev.* **44**, 643–656 (2015). <https://doi.org/10.1016/j.rser.2015.01.006>
- J. Pacio, T. Wetzel, Assessment of liquid metal technology status and research paths for their use as efficient heat transfer fluids in solar central receiver systems. *Sol. Energy* **93**, 11–22 (2013). <https://doi.org/10.1016/j.solener.2013.03.025>
- C. Wang, H. Xie, L. Zhang, Y. Gong, G. Pastel, J. Dai, B. Liu, E.D. Wachsman, L. Hu, Universal soldering of lithium and sodium alloys on various substrates for batteries. *Adv. Energy Mater.* **8**, 1701963 (2018). <https://doi.org/10.1002/aenm.201701963>
- X.-H. Yang, S.-C. Tan, J. Liu, Thermal management of Li-ion battery with liquid metal. *Energy Convers. Manag.* **117**, 577–585 (2016). <https://doi.org/10.1016/j.enconman.2016.03.054>
- G. Bo, L. Ren, X. Xu, Y. Du, S. Dou, Recent progress on liquid metals and their applications. *Adv. Phys. X* **3**, 412–442 (2018). <https://doi.org/10.1080/23746149.2018.1446359>
- S.K. Lin, C.Y. Yeh, M.J. Wang, On the formation mechanism of solid-solution Cu-to-Cu joints in the Cu/Ni/Ga/Ni/Cu system. *Mater. Charact.* **137**, 14–23 (2018). <https://doi.org/10.1016/j.matchar.2018.01.020>
- T. Gancarz, Physical, thermal, mechanical properties, and microstructural characterization of Sn–9Zn–XGa alloys. *Metall. Mater. Trans. A* **47**, 326–333 (2016). <https://doi.org/10.1007/s11661-015-3235-3>
- H. Ye, S. Xue, J. Luo, Y. Li, Properties and interfacial microstructure of Sn–Zn–Ga solder joint with rare earth Pr addition. *Mater. Des.* **46**, 816–823 (2013). <https://doi.org/10.1016/j.matdes.2012.10.034>
- J. Saint, M. Morcrette, D. Larcher, J.M. Tarascon, Exploring the Li–Ga room temperature phase diagram and the electrochemical performances of the Li–Ga alloys vs. Li. *Solid State Ionics* **176**, 189–197 (2005). <https://doi.org/10.1016/j.ssi.2004.05.021>
- S. Terlicka, A. Dębski, W. Gašior, Thermodynamic description of the Ga–Li–Zn system. *Thermochim. Acta* **659**, 66–73 (2018). <https://doi.org/10.1016/j.tca.2017.10.004>
- T. Gancarz, G. Cempura, Characterization of ZnAl cast alloys with Li addition. *Mater. Des.* **104**, 51–59 (2016). <https://doi.org/10.1016/j.matdes.2016.05.019>
- W. Gašior, B. Onderka, Z. Moser, A. Dębski, T. Gancarz, Thermodynamic evaluation of Cu–Li phase diagram from EMF measurements and DTA study. *Calphad* **33**, 215–220 (2009). <https://doi.org/10.1016/j.calphad.2008.10.006>
- Y. Li, Y. Du, T. Xu, H. Wu, X. Zhou, Z. Ling, Z. Zhang, Optimization of thermal management system for Li-ion batteries using phase change material. *Appl. Therm. Eng.* **131**, 766–778 (2018). <https://doi.org/10.1016/j.applthermaleng.2017.12.055>
- M. Sittig, *Sodium: its manufacture, properties and uses* (Reinhold Publishing Corporation, New York, 1956)
- T. Gancarz, Density, surface tension and viscosity of Ga–Sn alloys. *J. Mol. Liq.* **241**, 231–236 (2017). <https://doi.org/10.1016/j.molliq.2017.06.002>
- T. Gancarz, The physicochemical properties of liquid Ga–Zn alloys. *Fluid Phase Equilib.* **442**, 119–124 (2017). <https://doi.org/10.1016/j.fluid.2017.03.025>
- A. Dobosz, Y. Plevachuk, V. Sklyarchuk, B. Sokoliuk, T. Gancarz, Thermophysical properties of the liquid Ga–Sn–Zn eutectic alloy. *Fluid Phase Equilib.* **465**, 1–9 (2018). <https://doi.org/10.1016/j.fluid.2018.03.001>
- Y. Plevachuk, V. Sklyarchuk, S. Eckert, G. Gerbeth, R. Novakovic, Thermophysical properties of the liquid Ga–In–Sn eutectic alloy. *J. Chem. Eng. Data* **59**, 757–763 (2014). <https://doi.org/10.1021/je400882q>
- A. Dobosz, Y. Plevachuk, V. Sklyarchuk, B. Sokoliuk, T. Gancarz, The application of liquid metals in cooling systems: a study of the thermophysical properties of eutectic Ga–Sn–Zn with Al additions. *Int. J. Heat Mass Transf.* **126**, 414–420 (2018). <https://doi.org/10.1016/j.ijheatmasstransfer.2018.05.045>
- A. Dobosz, Y. Plevachuk, V. Sklyarchuk, B. Sokoliuk, O. Tkach, T. Gancarz, The thermophysical properties of eutectic Ga–Sn–Zn with In additions. *J. Mol. Liq.* **271**, 942–948 (2018). <https://doi.org/10.1016/j.molliq.2018.09.006>
- A. Dobosz, Y. Plevachuk, V. Sklyarchuk, B. Sokoliuk, O. Tkach, T. Gancarz, Liquid metals in high-temperature cooling systems: the effect of bi additions for the physicochemical properties of eutectic Ga–Sn–Zn. *J. Chem. Eng. Data* **64**, 404–411 (2019). <https://doi.org/10.1021/acs.jced.8b00519>
- T. Gancarz, W. Gašior, H. Henein, Physicochemical properties of Sb, Sn, Zn, and Sb–Sn system. *Int. J. Thermophys.* **34**, 250–266 (2013). <https://doi.org/10.1007/s10765-013-1407-1>
- T. Gancarz, W. Gašior, H. Henein, The discharge crucible method for making measurements of the physical properties of melts: an overview. *Int. J. Thermophys.* **35**, 1725–1748 (2014). <https://doi.org/10.1007/s10765-014-1748-4>
- T. Gancarz, Density, surface tension and viscosity of liquid ZnAl+X (X=Li, Na, Si) alloys. *Fluid Phase Equilib.* **427**, 97–103 (2016). <https://doi.org/10.1016/j.fluid.2016.06.045>
- T. Gancarz, Physicochemical properties of Sb–Sn–Zn alloys. *J. Electron. Mater.* **43**, 4374–4385 (2014). <https://doi.org/10.1007/s11664-014-3320-1>
- Y. Plevachuk, V. Sklyarchuk, Electrophysical measurements for strongly aggressive liquid semiconductors. *Meas. Sci. Technol.* **12**, 23–26 (2001). <https://doi.org/10.1088/0957-0233/12/1/303/meta>
- V. Sklyarchuk, Y. Plevachuk, A modified steady state apparatus for thermal conductivity measurements of liquid metals and

- semiconductors. *Meas. Sci. Technol.* **16**, 467–471 (2005). <https://doi.org/10.1088/0957-0233/16/2/019/meta>
29. D. Li, S. Fürtauer, H. Flandorfer, D.M. Cupid, Thermodynamic assessment and experimental investigation of the Li–Sn system. *Calphad* **47**, 181–195 (2014). <https://doi.org/10.1016/j.calphad.2014.09.002>
30. Y. Liang, Z. Du, C. Guo, C. Li, Thermodynamic modeling of the Li–Zn system. *J. Alloys Compd.* **455**, 236–242 (2008). <https://doi.org/10.1016/j.jallcom.2007.01.154>
31. T. Gancarz, P. Bobrowski, S. Pawlak, N. Schell, R. Chulist, K. Janik, Wetting of Sn–Zn–Ga and Sn–Zn–Na alloys on Al and Ni substrate. *J. Electron. Mater.* **47**, 49–60 (2017). <https://doi.org/10.1007/s11664-017-5791-3>
32. M.J. Assael, I.J. Armyra, J. Brillo, S.V. Stankus, J. Wu, W.A. Wakeham, Reference data for the density and viscosity of liquid cadmium, cobalt, gallium, indium, mercury, silicon, thallium, and zinc. *J. Phys. Chem. Ref. Data* **41**, 033101 (2012). <https://doi.org/10.1063/1.4729873>
33. J. Priede, A. Cramer, A. Bojarevics, A.Y. Gelfgat, P.Z. Bar-yoseph, A.L. Yarin, G. Gerbeth, Experimental and numerical study of anomalous thermocapillary convection in liquid gallium. *Phys. Fluids* **11**, 3331–3339 (1999). <https://doi.org/10.1063/1.870192>
34. K.C. Mills, Y.C. Su, Review of surface tension data for metallic elements and alloys: part 1–pure metals. *Int. Mater. Rev.* **51**, 329–351 (2006). <https://doi.org/10.1179/174328006X102510>
35. Yu. Plevachuk, V. Sklyarchuk, W. Hoyer, I. Kaban, Electrical conductivity, thermoelectric power and viscosity of liquid Sn-based alloys. *J. Mater. Sci.* **41**, 4632–4635 (2006). <https://doi.org/10.1007/s10853-006-0053-4>
36. Yu. Plevachuk, V. Sklyarchuk, Experimental investigations of phase equilibrium in liquid immiscible Zn–Pb alloys. *J. Mol. Liq.* **105**, 215–219 (2003). [https://doi.org/10.1016/S0167-7322\(03\)00056-4](https://doi.org/10.1016/S0167-7322(03)00056-4)
37. W.F. Calaway, The electrical resistivity of liquid lithium. *J. Less-Common Met.* **86**, 305–319 (1982)
38. Yu. Plevachuk, V. Sklyarchuk, A. Yakymovych, G. Gerbeth, Microsegregation in liquid Pb-based eutectics. *J. Non-Cryst. Solids* **354**, 4443–4447 (2008). <https://doi.org/10.1016/j.jnoncrysol.2008.06.068>
39. H. Neumann, Yu. Plevachuk, F. Allenstein, Investigation of Marangoni convection in monotectic melts by resistance measurements. *Mater. Sci. Eng. A* **361**, 155–164 (2003)
40. R.C. Martinelli, Heat transfer to molten metals. *Trans. ASME* **69**, 947–959 (1947)
41. R.N. Lyon, Liquid metal heat-transfer coefficients. *Chem. Eng. Prog.* **47**, 75–79 (1951)
42. R.A. Seban, T.T. Shimazaki, Heat transfer to a fluid flowing turbulently in a smooth pipe with walls at constant temperature. *Trans. ASME* **73**, 803–809 (1951)
43. B. Lubarsky, S.J. Kaufman, Review of experimental investigations of liquid-metal heat transfer, NACA TN 3336 (1955)
44. M.M. Sarafraz, J. Hart, E. Shrestha, H. Arya, M. Arjomandi, Experimental thermal energy assessment of a liquid metal eutectic in a microchannel heat exchanger equipped with a (10 Hz/50 Hz) resonator. *Appl. Therm. Eng.* **148**, 578–590 (2019). <https://doi.org/10.1016/j.applthermaleng.2018.11.073>
45. H. Mochizuki, Consideration on Nusselt numbers of liquid metals under low Peclet number conditions. *Nucl. Eng. Des.* **339**, 171–180 (2018). <https://doi.org/10.1016/j.nucengdes.2018.09.010>

Publisher's Note Springer Nature remains neutral with regard to jurisdictional claims in published maps and institutional affiliations.